



Long-term carbon dioxide sequestration by concretes with supplementary cementitious materials under indoor and outdoor exposure: Assessment as per a standardized model

Akli Younsi

► To cite this version:

Akli Younsi. Long-term carbon dioxide sequestration by concretes with supplementary cementitious materials under indoor and outdoor exposure: Assessment as per a standardized model. *Journal of Building Engineering*, 2022, 51, pp.104306. 10.1016/j.jobbe.2022.104306 . hal-03636488

HAL Id: hal-03636488

<https://hal.science/hal-03636488>

Submitted on 22 Jul 2024

HAL is a multi-disciplinary open access archive for the deposit and dissemination of scientific research documents, whether they are published or not. The documents may come from teaching and research institutions in France or abroad, or from public or private research centers.

L'archive ouverte pluridisciplinaire **HAL**, est destinée au dépôt et à la diffusion de documents scientifiques de niveau recherche, publiés ou non, émanant des établissements d'enseignement et de recherche français ou étrangers, des laboratoires publics ou privés.



Distributed under a Creative Commons Attribution - NonCommercial 4.0 International License

Long-term carbon dioxide sequestration by concretes with supplementary cementitious materials under indoor and outdoor exposure: Assessment as per a standardized model

Akli Younsi

La Rochelle University, LaSIE UMR CNRS 7356, Avenue Michel Crépeau, 17042 La Rochelle Cedex 1, France

E-mail address: akli.younsi@univ-lr.fr

Postal address: La Rochelle University, LaSIE UMR CNRS 7356, Avenue Michel Crépeau, 17042 La Rochelle Cedex 1, France

ABSTRACT

An experimental study was carried out on concretes designed with an ordinary Portland cement (CEM I 52.5 N), blended cements containing 23 wt.% fly ash (CEM II/B-V 32.5 R) or 82 wt.% ground granulated blast-furnace slag (CEM III/C 32.5 N), and partial substitutions of CEM I with fly ash (30 wt.%) or ground granulated blast-furnace slag (30 and wt.75 %). Measurements were carried out on Ø11X22 cm specimens after 10.8 years of exposure, under indoor and outdoor exposure, to determine their carbonation rates and degrees of carbonation. The objective was to compare CO₂ uptake calculated with the parameters measured experimentally to that calculated with parameters defined by a standardized model commonly used by construction engineering (EN 16757 model). The comparison showed that the model: (i) underestimates the carbonation rate (up to 61 %), (ii) underestimates the degree of carbonation under indoor exposure (up to 49 %) and overestimates it under outdoor exposure (up to 78 %), and (iii) considerably underestimates the maximum theoretical CO₂ uptake (up to 77 %) for high ground granulated blast-furnace slag content. Consequently, the model underestimates the CO₂ uptake under indoor exposure (up to 86 %). However, the comparison showed a better correlation under outdoor exposure. Based on these results, some adjustments to the parameters defined by the standardized model were suggested to better account for effects of exposure conditions and supplementary cementitious materials, which should improve the CO₂ uptake assessment.

Keywords: Cement substitution; Supplementary cementitious material; Low-carbon concrete; Indoor/Outdoor exposure; EN 16757 model; CO₂ uptake assessment

1. Introduction

Cement industry is a major contributor to global anthropogenic emissions of greenhouse gases (GHGs), especially carbon dioxide (CO₂) [1,2], which are the main source of global warming [3,4]. This industrial sector accounts for approximately 7.4 % of global CO₂ emissions [1,2,5–8] since production of 1 kg of cement releases 0.5 – 0.7 kg of CO₂ into atmosphere [2,4]. As cement is an essential component of concrete, its production is responsible for at least 70 % of GHGs from manufacture of concrete [9].

To mitigate CO₂ emissions from concrete manufacturing, cement and concrete industries have implemented several solutions such as using supplementary cementitious materials (SCMs) as partial substitution of clinker, the main component of Portland cement, during cement production, or cement during concrete manufacturing [4,6,9–11]. The use of industrial by-products, such as fly ash (FA) or ground granulated blast-furnace slag (GGBFS), which are among the most widely used SCMs in concrete [10], limits both systematic use of natural resources and landfill by recycling these by-products, and reduces CO₂ emissions from manufacture of concrete by up to 22 % [12].

From a life cycle assessment (LCA) point of view, considering only CO₂ emissions from concrete manufacturing has become insufficient to establish a more complete carbon footprint since concrete binds CO₂ through the process of carbonation. With its ability to sequester atmospheric CO₂, carbonation constitutes an important carbon sink that should be better considered in life cycle inventory of concrete [5,7–10,13–20].

Carbonation of a cementitious material is a natural aging phenomenon that has been widely studied in literature [9,13,14,17,18,21–29]. It is a process during which CO₂ diffuses from the atmosphere into the porosity of the material and reacts with carbonatable products. The latter are essentially hydration products, whose nature and structure depend mainly on nature of

binder, such as calcium hydroxide (Portlandite), different structures of calcium silicate hydrate (C-S-H) and ettringite, and some anhydrous phases of clinker, namely tricalcium silicate (C_3S) and dicalcium silicate (C_2S) [25]. Chemical reactions occurring during carbonation can be described, for simplicity, as a conversion of calcium oxide (CaO) to calcium carbonate ($CaCO_3$) [7–9,13,14,17–20,23,25,26,29]. According to durability of reinforced concrete, chemical reactions involving CO_2 lower the pH of concrete pore solution, which increases the risk of rebar corrosion. In this case, carbonation is considered as a degradation phenomenon [7,9,13,17,18,20,23,25–29]. According to environmental impact, the chemical reactions bind CO_2 within the concrete. In this case, carbonation is considered as a phenomenon that allows mitigating CO_2 emissions from concrete manufacturing [5,7–10,13–20].

Carbonation process of a cementitious material depends on a multitude of parameters that can be classified into two categories: intrinsic parameters which are characteristics (such as nature of binder [23–25,27–29]) and properties of the material, and extrinsic parameters relating mainly to the surrounding environment, such as duration and type of curing conditions [14,22–29], and carbonation conditions [13,17,18,26–29]. Interactions between all these parameters determine their actual effect on carbonation.

Curing a cementitious material consists in keeping it, at early age, at temperature and humidity conditions, such as under water, that favor the hydration of its binder [14,22,23,28,29], and thus lead to a material with low porosity [22,23,28], fine microstructure [23,28], and high amount of carbonatable products (hydration products) [28] within the surface layer (the skin). This slows down the progress of carbonation front (carbonation rate) [14,22,28,29] but enhances the carbonation reactions (bound CO_2 content and degree of carbonation) within the carbonated zone [13,17,18]. Moreover, resistance against carbonation increases with increasing curing duration [14,22–29], especially for materials with GGBFS

that are very sensitive to curing [14,23–25].

Carbonation conditions are known to significantly affect carbonation process [13,17,18,26–29], thus CO₂ uptake [13,17,18]. Compared to indoor exposure, outdoor exposure was found to decrease carbonation rate due to precipitation that keeps concrete porosity often close to saturation [28,29], and to increase bound CO₂ content and degree of carbonation because of high humidity in porosity due to precipitation [13,17,18].

In literature, there are some empirical calculation methods for determination of CO₂ uptake by cementitious materials [8]. However, the most used model, especially by European construction engineering, is the standardized model “EN 16757 model” [10,13,14,16–20,30]. The latter allows assessing CO₂ uptake, denoted Uptake, occurring during a period t by using Eq. (1):

$$\text{Uptake}(t) = k\sqrt{t} \cdot B \cdot U \cdot D \quad (1)$$

with: k is the carbonation rate. B is the binder content. U is the maximum theoretical CO₂ uptake in totally carbonated concrete. D is the degree of carbonation. The model defines k and D as tabulated values by considering exposure conditions and some concrete properties, and U by assuming that only CaO supplied by clinker reacts with CO₂. However, this approach for the definition of U is not consistent with literature which shows that CaO supplied by SCMs, especially GGBFS, also reacts with CO₂ [13,17,18]. Moreover, the tabulated values of both k and D should be checked with experimental values measured over a realistic and sufficiently long period, especially on concretes with SCMs.

The novelty of this work consists in: (i) readjusting the definition of U by assuming that all CaO supplied by binder, i.e., both clinker and SCMs, reacts with CO₂, and (ii) measuring values of k and D through an experimental campaign over a relatively long period. The study

was carried out on concretes designed with an ordinary Portland cement (CEM I), blended cements containing FA (CEM II/B-V) or GGBFS (CEM III/C), and partial substitutions of CEM I with FA or GGBFS. Concretes were demolded 24 h after casting and exposed under indoor and outdoor conditions for 10.8 years. During the exposure period, progress of carbonation front was monitored by regular carbonation measurements by phenolphthalein spraying to assess k . At the end of the exposure period, bound CO_2 content was determined by thermogravimetric analysis (TGA) to assess D . Finally, Uptake calculated with the parameters measured experimentally was compared to that calculated with the parameters of the standardized model. The objective was to suggest adjustments to the model, which should improve the CO_2 uptake assessment.

2. Materials

2.1. Raw materials

The six concretes studied were designed with three cements as per [31]: an ordinary Portland cement CEM I 52.5 N from Lafarge France, a fly ash cement CEM II/B-V 32.5 R from CCB Belgium, and a ground granulated blast-furnace slag cement CEM III/C 32.5 N from Calcia France. Two SCMs were used: a silico-aluminous fly ash (FA) from Surschiste France as per [32], and a ground granulated blast-furnace slag (GGBFS) from Ecocem Netherlands as per [33]. Other components were used: a siliceous sand (0/4 mm) and two crushed diorite gravels (6/10 and 10/14 mm) from HeidelbergCement France as per [34], and a polycarboxylate superplasticizer Fluid Optima 206[®] from Chryso France as per [35]. Some physical properties and chemical composition of the cementitious materials used are shown in Table 1.

Table 1

Some physical properties and chemical composition [wt.%] of the cements and SCMs used.

	CEM I	CEM II	CEM III	FA	GGBFS
Blaine surface [cm ² /g]	3400	3247	4280	4050	4500
Density [g/cm ³]	3.11	2.89	2.90	2.21	2.89
Clinker	95	73	15		
Limestone	5	4	3		
SCM	0	23	82		
CaO	64.8	48.9	45.1	5.2	41.5
SiO ₂	20.5	27.4	32.0	55.3	33.3
Al ₂ O ₃	4.5	9.0	10.3	25.2	12.5
Fe ₂ O ₃	2.7	3.4	0.8	6.4	0.4
SO ₃	3.5	2.8	2.9	0.5	0.2
MgO	1.5	2.0	6.1	0.9	7.0
K ₂ O	0.8	1.3	0.5	0.6	0.5
Na ₂ O	0.1	0.2	0.2	0.1	0.3

2.2. Concrete mixtures

Table 2 summarizes the proportions used in the six concrete mixtures studied. C I was designed with CEM I as per a usual industrial composition whose mix proportions were adjusted to achieve a minimum slump of 160 mm and a minimum characteristic 28-day compressive strength of 25 MPa, i.e., a consistency class S 4 and a compressive strength class C 25/30 as per [36]. The other five mixtures were designed from C I by varying the nature and amount of binder. Moreover, their compositions were readjusted to achieve the same consistency and compressive strength classes than C I. C II was designed with CEM II, C III with CEM III, F 30 with 30 wt.% substitution of CEM I with FA, S 30 with 30 wt.% substitution of CEM I with GGBFS, and S 75 with 75 wt.% substitution of CEM I with GGBFS.

Concrete mixtures were cast into Ø11X22 cm molds (4 molds per concrete) as per [37] and stored in a room at 20 ± 1 °C and 55 ± 5 % RH for 24 h, one of the durations usually used on construction sites.

Table 2

Mix proportions [kg/m³].

	C I	C II	C III	F 30	S 30	S 75
Cement	303	321	361	241	219	103
SCM	0	0	0	103	94	310
Sand	855	855	839	824	848	816
Gravel 6/10	211	211	207	204	209	201
Gravel 10/14	875	875	859	844	868	836
Effective water	182	175	175	182	182	170
Superplasticizer	1.36	1.00	1.00	1.75	0.26	1.89

2.3. Concrete properties

Some concrete properties required for this study are shown in Table 3. The binder content, denoted B [kg_{binder}/m³_{concrete}], is the sum of contents of cement and SCM (Table 2). The binder content, denoted b [-], is the ratio between B and the sum of contents of all constituents. The clinker content in binder, denoted c_1 [-], is that of CEM I, CEM II and CEM III (Table 1) for C I, C II and C III, respectively. For F 30, S 30 and S 75, c_1 is the clinker content in CEM I (0.95) multiplied by CEM I content in binder (Table 3). The clinker content in concrete is the binder content b multiplied by the clinker content in binder c_1 . The calcium oxide (CaO) content in binder, denoted CaO_b [-], is that of CEM I, CEM II and CEM III (Table 1) for C I, C II and C III, respectively. For F 30, S 30 and S 75, CaO_b is the sum of CaO content in CEM I (0.648) multiplied by CEM I content in binder (Table 3) and CaO content in SCM (Table 1) multiplied by SCM content in binder (Table 3). The CaO

content in concrete is the binder content b multiplied by the CaO content in binder CaO_b .

Table 3

Some properties of the concretes studied.

	C I	C II	C III	F 30	S 30	S 75
28-day compressive strength [MPa]	36	32	34	33	36	40
SCM content in binder [wt.%]	0	23	82	30	30	75
CEM I content in binder [wt.%]	100	0	0	70	70	25
Binder content (B) [kg/m ³]	303	321	361	344	313	413
Binder content (b) [wt.%]	12.5	13.2	14.8	14.3	12.9	16.9
Clinker content in binder (c_l) [wt.%]	95	73	15	67	67	24
Clinker content in concrete [wt.%]	11.9	9.6	2.2	9.6	8.6	4.1
CaO content in binder (CaO_b) [wt.%]	64.8	48.9	45.1	46.9	57.8	47.3
CaO content in concrete [wt.%]	8.1	6.5	6.7	6.7	7.5	8.0

3. Methods

3.1. Exposure procedure

The Ø11X22 cm specimens were demolded 24 h after casting and exposed under indoor and outdoor conditions for 10.8 years. The indoor exposure was carried out in a room where the average annual temperature was $\approx 19^\circ\text{C}$, the relative humidity $\approx 54\%$ and the CO_2 concentration $\approx 0.042\%$. The outdoor exposure was carried out on an experimental platform located within the La Rochelle University campus (French Atlantic coast) where the average annual temperature was $\approx 12^\circ\text{C}$, the relative humidity $\approx 76\%$ and the CO_2 concentration $\approx 0.038\%$. Measurements were carried out using a Vaisala HM 34[®] handheld digital instrument for temperature and relative humidity, and a Wittgas RLA 100[®] instrument for CO_2 concentration.

3.2. Phenolphthalein spraying

After 1, 6 and 10.8 years of exposure, for each concrete, two Ø11X5 cm samples, saw-cut from the Ø11X22 cm specimens, were split in half, and the split sections were sprayed with a pH indicator solution, namely phenolphthalein, to determine their carbonation depths as per [37]. It is commonly assumed that the zone that remains colorless ($pH < 9$) is totally carbonated, while the zone that turns pink ($pH > 9$) is not carbonated (Fig. 1).

3.3. Thermogravimetric analysis

Immediately after spraying phenolphthalein at 10.8 years, concrete powders were taken by drilling, using a Ø4 mm drill bit, from the center of both totally carbonated ($pH < 9$) and non-carbonated ($pH > 9$) zones of the split sections, as shown in Fig. 1. After that, the powders were tested by thermogravimetric analysis (TGA) using a Setaram Setsys Evolution® device. Measurements were carried out on ≈ 150 mg powders in argon atmosphere at 10 °C/min from 25 to 1000 °C to determine their bound CO_2 contents [38].

Bound CO_2 content expressed by mass of binder, denoted CO_2 [kg_{CO_2}/kg_{binder}], was determined by Eq. (2):

$$CO_2 = \left(\frac{\Delta m}{m \cdot b} \right)_{pH < 9} - \left(\frac{\Delta m}{m \cdot b} \right)_{pH > 9} \quad (2)$$

with: Δm [mg] is the mass loss of powder measured by TGA between ≈ 530 and ≈ 950 °C

[39]. These two temperatures were readjusted for each powder using the derivative thermogravimetry DTG, where the main peak associated with CaCO_3 decarbonation appears at 600 – 800 °C [40]. m [mg] is the mass of powder tested by TGA. b [-] is the binder content (Table 3). It should be noted that CO_2 quantified in the non-carbonated zone, i.e., $\left(\frac{\Delta m}{m \cdot b}\right)_{pH > 9}$, results from decarbonation of calcium carbonate (CaCO_3) supplied by concrete constituents. It must thus be removed to only quantify CO_2 bound by carbonatable products.

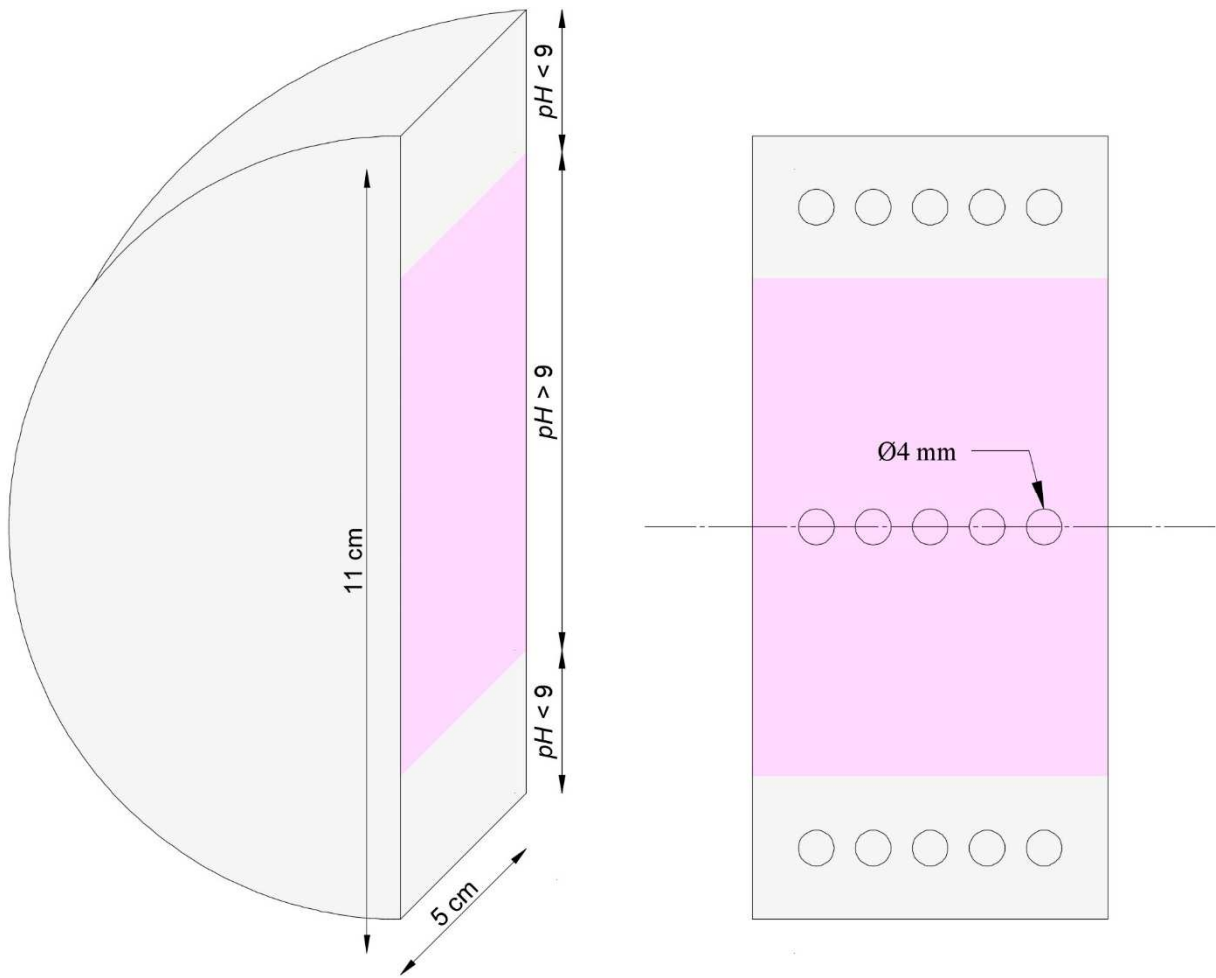


Fig. 1. Schematic representation of the powder sampling.

4. Results and discussion

The following sections report the results obtained and discuss: (i) the comparison between parameters measured experimentally and those defined by the standardized model, (ii) the comparison between parameters measured under indoor exposure and those measured under outdoor exposure, and (iii) the effect of nature of binder. It should be noted that the term “model” will refer to the standardized model and parameters as per this model will take the index “St”. The index “Ex” will refer to parameters measured experimentally.

4.1. Carbonation rate “ k ”

The model defines carbonation rate, denoted k_{St} [m/year^{0.5}], by considering compressive strength (Table 3), type of SCM used (FA or GGBFS) and its content in binder (Table 3), and exposure conditions (indoor or outdoor).

To check experimentally the tabulated values of k_{St} , a carbonation rate, denoted k_{Ex} [m/year^{0.5}], was determined from carbonation depths revealed by phenolphthalein, by using a linear regression through zero, i.e., by considering a square root of time relationship, as shown in Eq. (3):

$$X_c(t) = k_{Ex}\sqrt{t} \quad (3)$$

with: $X_c(t)$ [m] is the carbonation depth measured at a time t [year].

A comparison between k_{Ex} and k_{St} is shown in Fig. 2a. k_{Ex} is higher than k_{St} (relative

deviation up to 61 %). This means that the model underestimates carbonation rate. The tabulated values of k_{st} should then be readjusted (increased) to better account for effects of both exposure conditions and nature of binder. Andrade, who assessed carbonation rates with high dispersions compared to those introduced by the model, suggested defining adjustments per country for k_{st} due to the diversity of exposure conditions and cements used [17].

Fig. 2b shows a comparison between carbonation rate measured under indoor exposure (k_{ExIn}) and that measured under outdoor exposure (k_{ExOut}). k_{ExIn} is higher than k_{ExOut} (relative deviation up to 76 %). This means that outdoor exposure decreases carbonation rate, which is consistent with literature [28,29]. Precipitation is known to keep concrete porosity often close to saturation. In this case, CO_2 diffuses only through the pore solution, i.e., more slowly than in air. This significantly hampers carbonation that occurs when porosity is sufficiently dry up to the carbonation depth reached before precipitation. Hence, under outdoor exposure, carbonation is essentially governed by length and frequency of wetting/drying periods, while under indoor exposure, concrete porosity is often partially saturated [28,29].

Whatever the exposure conditions, C I exhibits the lowest carbonation rate while C III the highest one. This is expected since C I contains the highest clinker content while C III the lowest one (Table 3). Increasing clinker content is known to increase amount of carbonatable products (hydration products) and to densify microstructure, which enhances resistance against carbonation.

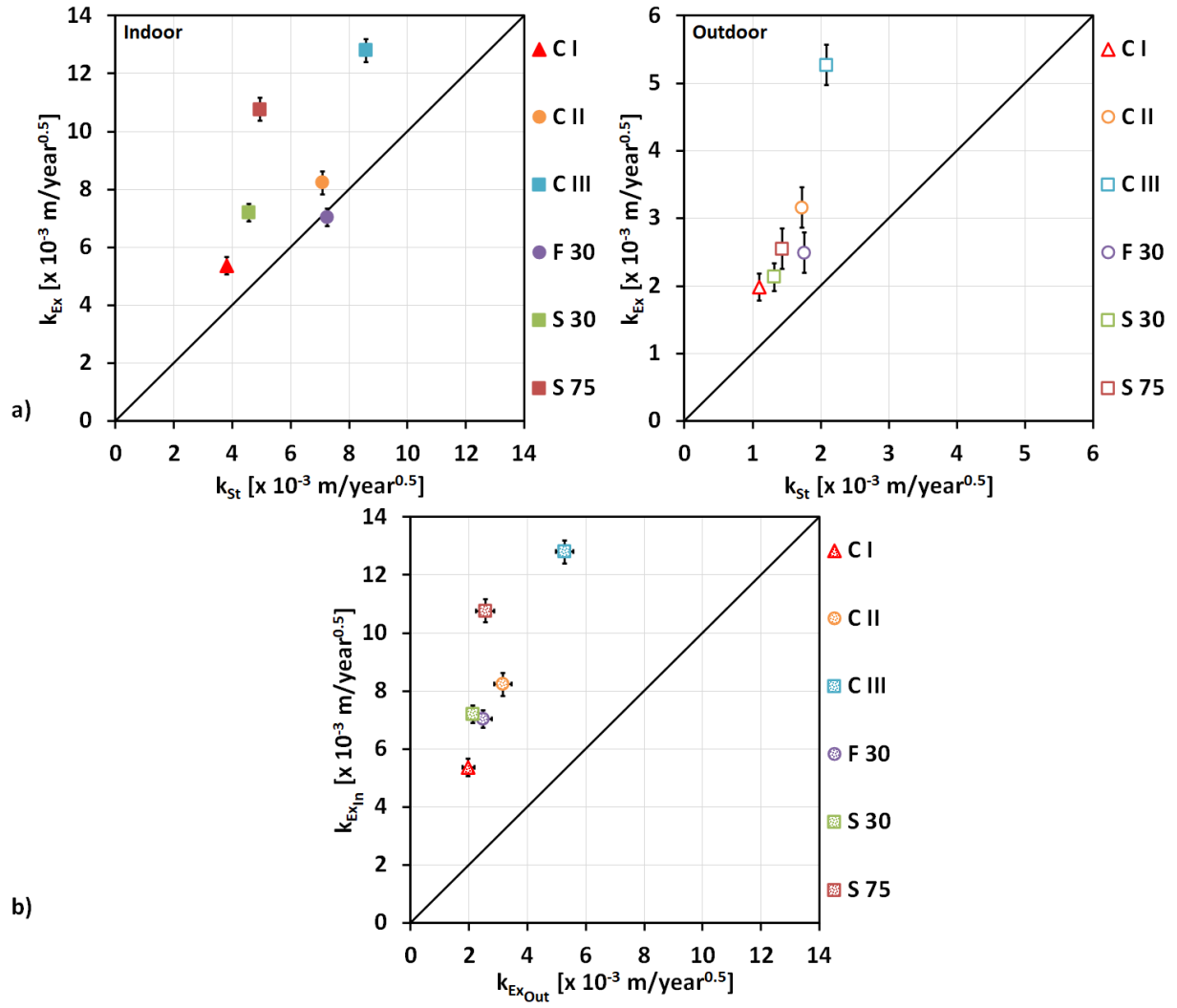


Fig. 2. (a) Carbonation rates measured (k_{Ex}) *versus* tabulated values of the model (k_{St}). (b) Carbonation rates measured under indoor exposure (k_{ExIn}) *versus* values measured under outdoor exposure (k_{ExOut}).

4.2. Maximum theoretical CO_2 uptake “U”

The model introduces the concept of maximum theoretical CO_2 uptake in totally carbonated concrete, denoted $U_{St} [kg_{CO_2}/kg_{binder}]$, based on a conservative approach which assumes that only CaO supplied by clinker reacts with CO_2 . U_{St} is then defined as a function

of CaO content in clinker of Portland cement CEM I, using Eq. (4):

$$U_{St} = c_l \cdot CaO_{CEM\ I} \cdot \frac{M_{CO_2}}{M_{CaO}} \quad (4)$$

with: c_l [-] is the clinker content in binder (Table 3). $CaO_{CEM\ I}$ [-] is the CaO content in CEM I (Table 1). M_{CO_2} and M_{CaO} [kg/mol] are the molecular weights of CO_2 and CaO, respectively.

According to literature, CaO supplied by SCMs, especially GGBFS, also reacts with CO_2 [13,17,18]. A maximum theoretical CO_2 uptake in totally carbonated concrete, denoted U_{Ex} [kg $_{CO_2}$ /kg $_{binder}$], was thus defined by assuming that all CaO supplied by binder, i.e., both clinker and SCMs, reacts with CO_2 . Its expression is given by Eq. (5):

$$U_{Ex} = CaO_b \cdot \frac{M_{CO_2}}{M_{CaO}} \quad (5)$$

with: CaO_b [-] is the CaO content in binder (Table 3).

Fig. 3 shows a comparison between U_{Ex} and U_{St} . U_{Ex} is significantly higher than U_{St} for C III and S 75 with relative deviations of 77 and 68 %, respectively. In fact, for these concretes with very low clinker content (Table 3), considering only carbonation of CaO supplied by clinker leads to very low values of U_{St} . This means that the conservative approach of the model considerably underestimates the maximum theoretical CO_2 uptake for high GGBFS content.

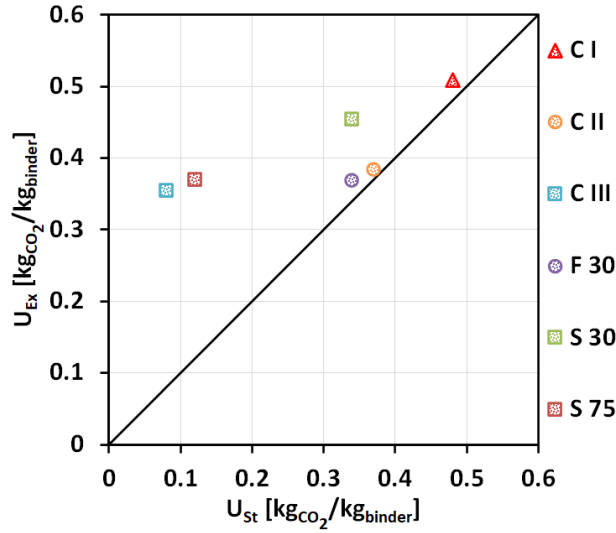


Fig. 3. Maximum theoretical CO₂ uptakes in totally carbonated concrete: values as per the definition of this study (U_{Ex}) *versus* values as per the definition of the model (U_{St}).

4.3. Degree of carbonation “D”

Degree of carbonation is the ratio between carbonated and available reactive CaO. It can be expressed as the ratio between bound CO₂ content expressed by mass of binder and maximum theoretical CO₂ uptake in totally carbonated concrete.

The model defines degree of carbonation, denoted D_{St} [-], by considering only exposure conditions (indoor or outdoor). The tabulated values of D_{St} are 0.40 and 0.85 for indoor and outdoor exposure, respectively.

Using the maximum theoretical CO₂ uptake which assumes that only CaO supplied by clinker reacts with CO₂, a degree of carbonation, denoted D_{U_{St}} [-], was defined by Eq. (6):

$$D_{U_{St}} = \frac{CO_2}{U_{St}} \quad (6)$$

Using the maximum theoretical CO₂ uptake which assumes that all CaO supplied by binder reacts with CO₂, a degree of carbonation, denoted D_{Ex} [-], was defined by Eq. (7):

$$D_{Ex} = \frac{CO_2}{U_{Ex}} \quad (7)$$

A comparison between D_{Ex} and D_{U_{St}} is shown in Fig. 4a. D_{Ex} is significantly lower than D_{U_{St}} for C III and S 75 with the same relative deviations observed with U_{Ex} and U_{St} (Fig. 3). D_{U_{St}} for these concretes approaches or even exceeds 1. This suggests that CaO supplied by GGBFS also reacts with CO₂, which is in accordance with literature [13,17,18]. The conservative approach of the model, which considerably underestimates the maximum theoretical CO₂ uptake for high GGBFS content (Fig. 3), should then be revised by readapting the definition of U_{St}, at least for concretes with GGBFS, to avoid aberrant degrees of carbonation (> 1).

Fig. 4b shows a comparison between D_{Ex} and D_{St}. D_{Ex} is higher than D_{St} under indoor exposure (relative deviation up to 49 %) and lower than D_{St} under outdoor exposure (relative deviation up to 78 %). This means that the model underestimates the degree of carbonation under indoor exposure and overestimates it under outdoor exposure. The tabulated values of D_{St} should then be revised to better account for effects of both exposure conditions and nature of binder.

A comparison between the degree of carbonation measured under indoor exposure (D_{ExIn}) and that measured under outdoor exposure (D_{ExOut}) is shown in Fig. 4c. D_{ExIn} is higher than D_{ExOut} (relative deviation up to 48 %). This means that outdoor exposure decreases the degree of carbonation, which is not consistent with the results presented by Andrade [17] who showed that outdoor exposure slightly increases the bound CO₂ content and degree of

carbonation because of high humidity in concrete porosity due to precipitation [13,17,18]. As mentioned previously, under outdoor exposure, carbonation process is highly dependent on length and frequency of wetting/drying periods [28,29]. The outdoor exposure was carried out under a moderate climate characterized by long periods of sunshine and wind. Although the average annual relative humidity is relatively high due to the proximity to the Atlantic Ocean, short periods of precipitation followed by rapid and frequent drying, due to sunshine and wind, could reduce the water content from the porosity within the carbonated zone, which could slightly hamper the carbonation reactions, thus could reduce the bound CO_2 content and degree of carbonation. Porosity however remains enough saturated to slow down the progress of carbonation front, i.e., the carbonation rate. Under indoor exposure, porosity remains often partially saturated, which favors both the carbonation reactions (degree of carbonation) and the progress of carbonation front (carbonation rate) [27].

Whatever the exposure conditions, C III and S 75 exhibit low degrees of carbonation despite their high carbonation rates (Fig. 2b). This suggests that there is no relationship between carbonation rate and degree of carbonation, which is consistent with literature [17,18]. Moreover, the degree of carbonation of C III is two times lower than that of F 30 despite their identical CaO contents (Table 3). A similar observation can be made with S 75 and C I. This suggests that even if CaO supplied by GGBFS reacts with CO_2 , hydrates produced by clinker seem to bind more CO_2 . According to literature, increasing GGBFS content decreases the Ca/Si ratio of C-S-H, which hampers their carbonation reactions [41]. This could explain the low degrees of carbonation noticed with C III and S 75.

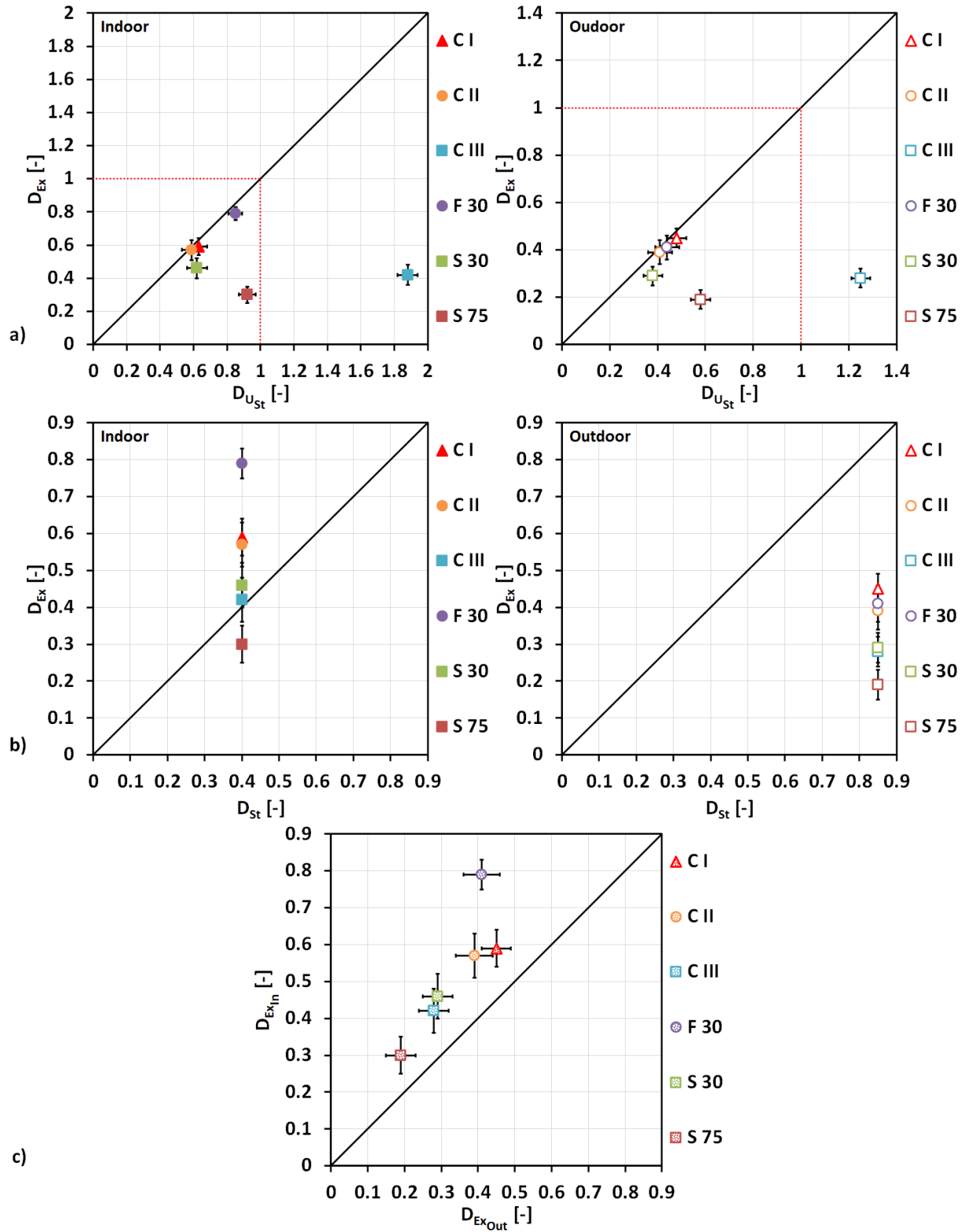


Fig. 4. (a) Degrees of carbonation expressed by U_{Ex} (D_{Ex}) *versus* values expressed by U_{St} (D_{Ust}). (b) Degrees of carbonation expressed by U_{Ex} (D_{Ex}) *versus* tabulated values of the

model (D_{St}). (c) Degrees of carbonation measured under indoor exposure (D_{ExIn}) *versus* values measured under outdoor exposure (D_{ExOut}).

4.4. CO₂ uptake “Uptake”

The model assesses CO₂ uptake, denoted $Uptake_{St}$ [kg_{CO₂}/m²_{concrete}], by Eq. (8):

$$Uptake_{St}(t) = k_{St}\sqrt{t} \cdot B \cdot U_{St} \cdot D_{St} \quad (8)$$

with: B [kg_{binder}/m³_{concrete}] is the binder content (Table 3).

For comparison, a CO₂ uptake, denoted $Uptake_{Ex}$ [kg_{CO₂}/m²_{concrete}], was calculated with the parameters measured experimentally, using Eq. (9):

$$Uptake_{Ex}(t) = k_{Ex}\sqrt{t} \cdot B \cdot U_{Ex} \cdot D_{Ex} \quad (9)$$

A comparison between $Uptake_{Ex}$ and $Uptake_{St}$ at $t = 10.8$ years is shown in Fig. 5a. It should be noted that due to the aberrant $D_{U_{St}}$ shown with C III (Fig. 4a), this degree of carbonation was not used to determine CO₂ uptake.

Under indoor exposure, $Uptake_{Ex}$ is higher than $Uptake_{St}$ (relative deviation up to 86 %). The model underestimates the CO₂ uptake because it underestimates the carbonation rate (Fig. 2b), the maximum theoretical CO₂ uptake (Fig. 3), and the degree of carbonation (Fig. 4b).

Under outdoor exposure, a better compensation between the overestimated degrees of carbonation, and the underestimated carbonation rates and maximum theoretical CO₂ uptakes,

allowed a better correlation between $\text{Uptake}_{\text{Ex}}$ and $\text{Uptake}_{\text{St}}$, except for C III (relative deviation of 73 %) due to huge differences between its k_{Ex} and k_{St} (Fig. 2a), and between its U_{Ex} and U_{St} (Fig. 3).

As suggested previously, readjusting D_{St} and k_{St} to better account for effects of both exposure conditions and nature of binder, and readapting the definition of U_{St} (mainly for high GGBFS content), should improve CO_2 uptake assessment by the model.

Fig. 5b shows a comparison between CO_2 uptake measured under indoor exposure ($\text{Uptake}_{\text{ExIn}}$) and that measured under outdoor exposure ($\text{Uptake}_{\text{ExOut}}$). $\text{Uptake}_{\text{ExIn}}$ is significantly higher than $\text{Uptake}_{\text{ExOut}}$ (relative deviation up to 85 %). This means that outdoor exposure decreases the CO_2 uptake, which is expected since it decreases both the degree of carbonation and the carbonation rate.

Whatever the exposure conditions, because of its low carbonation rate (Fig. 2b), C I exhibits lower CO_2 uptake than C II, C III and F 30.

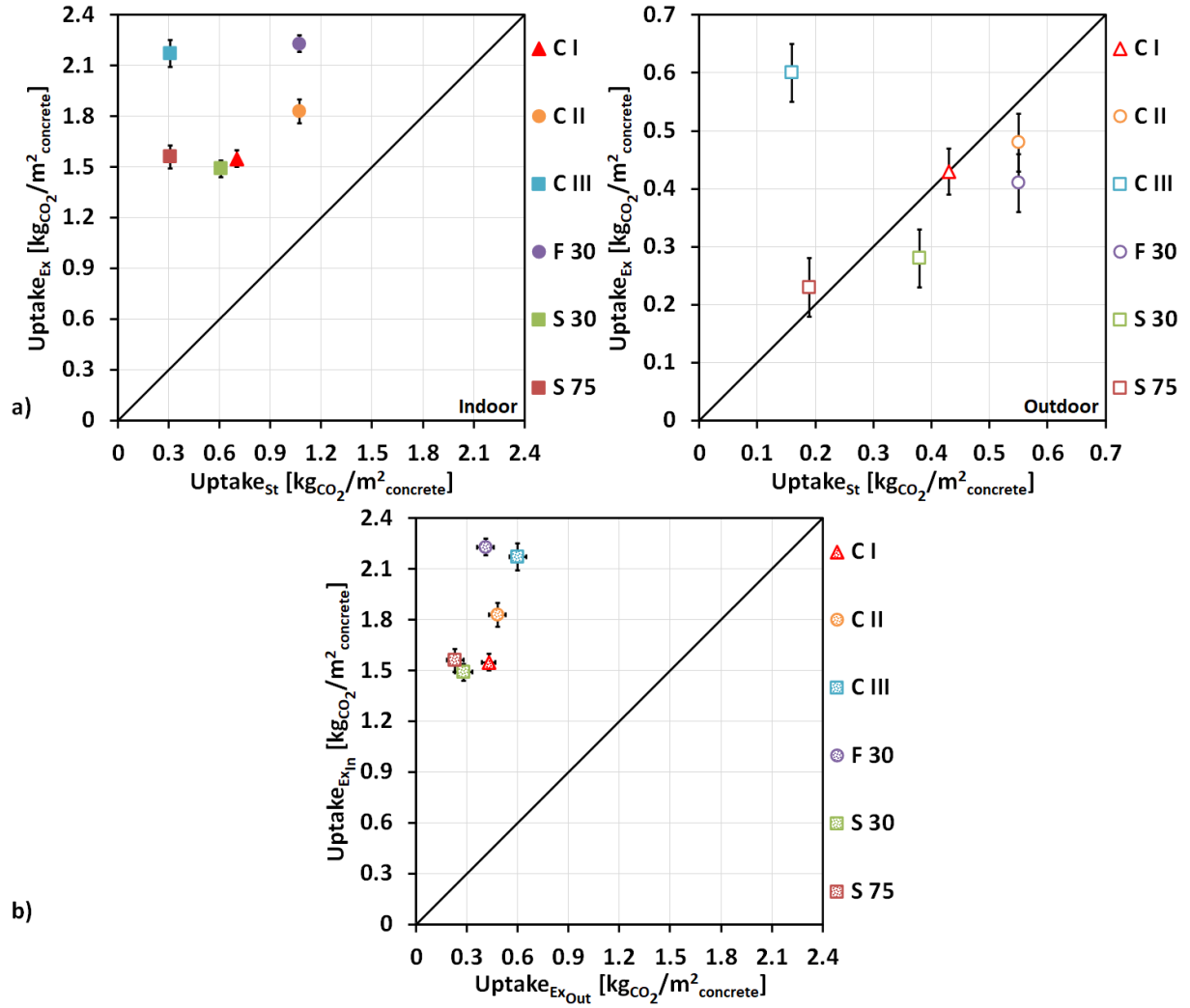


Fig. 5. (a) CO₂ uptakes calculated with parameters measured (Uptake_{Ex}) *versus* values calculated with the parameters of the model (Uptake_{St}). (b) CO₂ uptakes measured under indoor exposure (Uptake_{Ex_{In}}) *versus* values measured under outdoor exposure (Uptake_{Ex_{Out}}).

5. Conclusions

The main findings of the study can be summarized as follows:

- Concretes with high GGBFS content (75 and wt.82 %) exhibit low degrees of carbonation despite their high CaO content, suggesting that even if CaO supplied by GGBFS reacts with CO₂, clinker seems to bind more CO₂. Low Ca/Si ratio of C-S-H could explain this

finding.

- Compared to indoor exposure, outdoor exposure decreases the carbonation rate (up to 76 %), the degree of carbonation (up to 48 %), and thus the CO₂ uptake (up to 85 %).
- Comparison between carbonation rates measured and those defined by the model shows that the latter underestimates the carbonation rate (up to 61 %).
- Comparison between maximum theoretical CO₂ uptakes defined by assuming that all CaO supplied by binder reacts with CO₂ and those defined by the model shows that the model considerably underestimates this parameter (up to 77 %) for high GGBFS content. This leads to aberrant degrees of carbonation (> 1) for these concretes.
- Comparison between degrees of carbonation measured and those introduced by the model shows that the latter underestimates the degree of carbonation under indoor exposure (up to 49 %) and overestimates it under outdoor exposure (up to 78 %).
- Comparison between CO₂ uptakes calculated with the parameters measured and those calculated with parameters defined by the model shows that the latter underestimates the CO₂ uptake under indoor exposure (up to 86 %). A better correlation is however shown under outdoor exposure.

Based on these results, to improve the CO₂ uptake assessment, some adjustments need to be made to the model:

- Tabulated values of carbonation rate defined by the model should be readjusted to better account for effects of both exposure conditions and SCMs.
- Conservative approach of the model which assumes that only CaO supplied by clinker reacts with CO₂ should be revised by readapting the definition of maximum theoretical CO₂ uptake to avoid aberrant degrees of carbonation (> 1), mainly for high GGBFS content.
- Tabulated values of degree of carbonation defined by the model should be revised to

better consider effects of exposure and nature of binder. For instance, the value 0.40 for indoor exposure should be increased, while the value 0.85 for outdoor exposure should be reduced.

Declaration of competing interest

The author declares that he has no known competing financial interests or personal relationships that could have appeared to influence the work reported in this paper.

Acknowledgments

The author would like to acknowledge the French National Research Agency (ANR) for funding the *EcoBéton* project during which the concretes studied were designed, and the French National Federation of Public Works (FNTP) for funding part of the characterization by TGA.

References

- [1] Zhang, C.Y., Han, R., Yu, B., Wei, Y.M., 2018. Accounting process-related CO₂ emissions from global cement production under Shared Socioeconomic Pathways. *J. Clean. Prod.* 184, 451–465. <https://doi.org/10.1016/j.jclepro.2018.02.284>.
- [2] Wojtacha-Rychter, K., Kucharski, P., Smolinski, A., 2021. Conventional and Alternative Sources of Thermal Energy in the Production of Cement – An Impact on CO₂ Emission. *Energies* 14, 1539. <https://doi.org/10.3390/en14061539>.
- [3] Benhelal, E., Shamsaei, E., Rashid, M.I., 2021. Challenges against CO₂ abatement

- strategies in cement industry: a review. *J. Environ. Sci.* 104, 84–101.
<https://doi.org/10.1016/j.jes.2020.11.020>.
- [4] Nie, S., Zhou, J., Yang, F., Lan, M., Li, J., Zhang, Z., Chen, Z., Xu, M., Li, H., Sanjayan, J.G., 2022. Analysis of theoretical carbon dioxide emissions from cement production: Methodology and application. *J. Clean. Prod.* 334, 130270.
<https://doi.org/10.1016/j.jclepro.2021.130270>.
- [5] Sanjuán, M.Á., Andrade, C., Mora, P., Zaragoza, A., 2020. Carbon dioxide uptake by cement-based materials: A Spanish case study. *Appl. Sci.* 10, 339.
<https://doi.org/10.3390/app10010339>.
- [6] Bouarroudj, M.E., Remond, S., Bulteel, D., 2020. Use of grinded hardened cement pastes as mineral addition for mortars. *J. Build. Eng.* 23, 101863.
<https://doi.org/10.1016/j.jobbe.2020.101863>.
- [7] Gupta, S., 2021. Carbon sequestration in cementitious matrix containing pyrogenic carbon from waste biomass: A comparison of external and internal carbonation approach. *J. Build. Eng.* 43, 102910. <https://doi.org/10.1016/j.jobbe.2021.102910>.
- [8] Kwon S.-J., Wang X.-Y., 2021. CO₂ uptake model of limestone-powder-blended concrete due to carbonation. *J. Build. Eng.* 38, 102176.
<https://doi.org/10.1016/j.jobbe.2021.102176>.
- [9] Habert, G., Miller, S.A., John, V.M., Provis, J.L., Favier, A., Horvath, A., Scrivener, K.L., 2020. Environmental impacts and decarbonization strategies in the cement and concrete industries. *Nat. Rev. Earth Environ.* 1, 559–573.
<https://doi.org/10.1038/s43017-020-0093-3>.
- [10] Marinković, S., Carević, V., Dragaš, J., 2021. The role of service life in Life Cycle Assessment of concrete structures. *J. Clean. Prod.* 290, 125610.
<https://doi.org/10.1016/J.JCLEPRO.2020.125610>.

- [11] Bae, J.-H., Kim, S., Amr, I.T., Seo, J., Jang, D., Bamagain, R., Fadhel, B.A., Abu-Aisheh, E., Lee, H.K., 2022. Evaluation of physicochemical properties and environmental impact of environmentally amicable Portland cement/metakaolin bricks exposed to humid or CO₂ curing condition. *J. Build. Eng.* 47, 103831. <https://doi.org/10.1016/j.jobbe.2021.103831>.
- [12] Flower, D.J.M., Sanjayan, J.G., 2007. Green house gas emissions due to concrete manufacture. *Int. J. Life Cycle Assess.* 12, 282–288. <https://doi.org/10.1065/lca2007.05.327>.
- [13] Andrade, C., Sanjuán, M.Á., 2018. Updating Carbon Storage Capacity of Spanish Cements. *Sustainability* 10, 4806. <https://doi.org/10.3390/su10124806>.
- [14] Sanjuán, M.Á., Estévez, E., Argiz, C, 2019. Carbon Dioxide Absorption by Blast-Furnace Slag Mortars in Function of the Curing Intensity. *Energies* 12, 2346. <https://doi.org/10.3390/en12122346>.
- [15] Sanjuán, M.Á., Argiz, C., Mora, P., Zaragoza, A., 2020. Carbon dioxide uptake in the roadmap 2050 of the Spanish cement industry. *Energies* 13, 3452. <https://doi.org/10.3390/en13133452>.
- [16] Sanjuán, M.Á., Andrade, C., Mora, P., Zaragoza, A., 2020. Carbon Dioxide Uptake by Mortars and Concretes Made with Portuguese Cements. *Appl. Sci.* 10, 646. <https://doi.org/10.3390/app10020646>.
- [17] Andrade, C., 2020. Evaluation of the degree of carbonation of concretes in three environments. *Constr. Build. Mater.* 230, 116804. <https://doi.org/10.1016/j.conbuildmat.2019.116804>.
- [18] Andrade, C., Sanjuán, M.Á., 2021. Carbon dioxide uptake by pure Portland and blended cement pastes. *Dev. Built Environ.* 8, 100063. <https://doi.org/10.1016/j.dibe.2021.100063>.

- [19] AzariJafari, H., Guo, F., Gregory, J., Kirchain, R., 2021. Carbon uptake of concrete in the US pavement network. *Resour. Conserv. Recycl.* 167, 105397. <https://doi.org/10.1016/j.resconrec.2021.105397>.
- [20] Mäkikouri, S., Vares, S., Korpijärvi, K., Papakonstantinou, N., 2021. The Carbon Dioxide Emissions Reduction Potential of Carbon-Dioxide-Cured Alternative Binder Concrete. *Recent Prog. Mater.* 3, 1–34. <https://doi.org/10.21926/rpm.2102018>.
- [21] Sanjuán, M.Á., Andrade, C., Cheyrezy, M., 2003. Concrete carbonation tests in natural and accelerated conditions. *Adv. Cem. Res.* 15, 171–180. <https://doi.org/10.1680/adcr.2003.15.4.171>.
- [22] Fattuhi, N.I., 1988. Concrete carbonation as influenced by curing regime. *Cem. Concr. Res.* 18, 426–430. [https://doi.org/10.1016/0008-8846\(88\)90076-2](https://doi.org/10.1016/0008-8846(88)90076-2).
- [23] Sanjuán, M.Á., Piñeiro, A., Rodríguez, O., 2011. Ground granulated blast furnace slag efficiency coefficient (k value) in concrete. Applications and limits. *Mater. Constr.* 61, 303–313. <https://doi.org/10.3989/mc.2011.60410>.
- [24] Gruyaert, E., Heede, P.V.d., Belie, N.D., 2013. Carbonation of slag concrete: effect of the cement replacement level and curing on the carbonation coefficient–effect of carbonation on the pore structure. *Cem. Concr. Compos.* 35, 39–48. <https://doi.org/10.1016/j.cemconcomp.2012.08.024>.
- [25] Sanjuán, M.Á., Estévez, E., Argiz, C., del Barrio, D., 2018. Effect of curing time on granulated blast-furnace slag cement mortars carbonation. *Cem. Concr. Compos.* 90, 257–265. <https://doi.org/10.1016/j.cemconcomp.2018.04.006>.
- [26] Yoon, I.-S., Çopuroglu, O., Park, K.-B., 2007. Effect of global climatic change on carbonation progress of concrete. *Atmos. Environ.* 41, 7274–7285. <https://doi.org/10.1016/j.atmosenv.2007.05.028>.
- [27] Ekolü, S.O., 2016. A review on effects of curing, sheltering, and CO₂ concentration

- upon natural carbonation of concrete. *Constr. Build. Mater.* 127, 306–320.
<https://doi.org/10.1016/j.conbuildmat.2016.09.056>.
- [28] Ikotun, J.O., 2018. Effects of concrete quality and natural Johannesburg environment on concrete carbonation rate. *MATEC Web Conf.* 199, 02008.
<https://doi.org/10.1051/matecconf/201819902008>.
- [29] Otieno, M., Ikotun, J., Ballim, Y., 2020. Experimental investigations on the effect of concrete quality, exposure conditions and duration of initial moist curing on carbonation rate in concretes exposed to urban, inland environment. *Constr. Build. Mater.* 246, 118443. <https://doi.org/10.1016/j.conbuildmat.2020.118443>.
- [30] EN 16757 Standard, 2017. Sustainability of construction works – Environmental product declaration – Product Category Rules for concrete and concrete elements.
- [31] EN 197-1 Standard, 2011. Cement – Part 1: Composition, specifications and conformity criteria for common cements.
- [32] EN 450-1 Standard, 2012. Fly ash for concrete – Part 1: Definition, specifications and conformity criteria.
- [33] EN 15167-1 Standard, 2006. Ground granulated blast-furnace slag for use in concrete, mortar and grout – Part 1: Definitions, specifications and conformity criteria.
- [34] EN 13139 Standard, 2003. Aggregates for mortar.
- [35] EN 934-2+A1 Standard, 2012. Admixtures for concrete, mortar and grout – Part 2: Concrete admixtures – Definitions, requirements, conformity, marking and labelling.
- [36] EN 206/CN Standard, 2014. Concrete, specification, performance, production and conformity.
- [37] EN 12390-12 Standard, 2020. Testing hardened concrete – Part 12: Determination of the carbonation resistance of concrete – Accelerated carbonation method.
- [38] Tchakouté, H.K., Rüschler, C.J., Kong, S., Ranjbar, N., 2016. Synthesis of sodium

- waterglass from white rice husk ash as an activator to produce metakaolin based geopolymer cements. *J. Build. Eng.* 6, 252–261. <https://doi.org/10.1016/j.jobbe.2016.04.007>.
- [39] Villain, G., Thiery, M., Platret, G., 2007. Measurement Methods of Carbonation Profiles in Concrete: Thermogravimetry, Chemical Analysis and Gammadensimetry. *Cem. Concr. Res.* 37, 1182–1192. <https://doi.org/10.1016/j.cemconres.2007.04.015>.
- [40] Liu, J., Liu, J., Fan, W., Jin, H., Zhu, J., Huang, Z., Xing, F., Sui, T., 2022. Investigation on water sorptivity and micro properties of concrete: Effect of supplementary cementitious materials, seawater, sea-sand and water-binder ratio. *J. Build. Eng.* <https://doi.org/10.1016/j.jobbe.2022.104153>.
- [41] Li, J., Yu, Q., Huang, H., Yin, S., 2019. Effects of Ca/Si ratio, aluminum and magnesium on the carbonation behavior of calcium silicate hydrate. *Materials*. 12, 1268. <https://doi.org/10.3390/ma12081268>.